Direct observation of fast proton transfer: femtosecond photophysics of 3-hydroxyflavone

ARTICLE *in* CHEMINFORM · APRIL 1992

Impact Factor: 0.74 · DOI: 10.1021/j100188a009

3 AUTHORS, INCLUDING:

Linda A. Peteanu
Carnegie Mellon University
66 PUBLICATIONS **3,393** CITATIONS

Direct Observation of Fast Proton Transfer: Femtosecond Photophysics of 3-Hydroxyflavone

Benjamin J. Schwartz, Linda A. Peteanu, and Charles B. Harris*

Department of Chemistry, University of California, Berkeley, Berkeley, California 94720
(Received: November 26, 1991)

We report the first investigation of the fast excited-state intramolecular proton transfer of 3-hydroxyflavone. Picosecond stimulated emission and transient absorption spectroscopy demonstrate that the tautomer formation can be monitored by 620-nm transient absorption. The excited-state proton transfer was studied at 620 nm with femtosecond time resolution, and determined to be 240 ± 50 fs in a nonpolar solvent environment. The fast excited-state proton transfer in methanol solution, however, was faster than the 125-fs instrument response. A simple model describing the mechanism of the fast excited-state proton transfer of 3-hydroxyflavone in different solvents is presented.

I. Introduction

Proton-transfer reactions are one of the simplest chemical transformations. Despite their chemical simplicity, subtleties in the shapes of the relevant potential energy surfaces, quantum mechanical tunneling effects, and extremely high reaction rates have made these reactions difficult to understand.[1] Many molecules with adjacent acidic and basic functional groups are capable of undergoing intramolecular proton transfer. In many cases, the proton affinities of these sites change upon photoexcitation,[2] leading to excited-state proton transfer (ESPT), and indeed, with recent advances in ultrafast laser technologies, significant progress has been made in understanding these reactions.

One of the most widely studied molecules which exhibits ESPT is 3-hydroxyflavone (3HF).[3-15] Sengupta and Kasha first proposed[3] that 3HF undergoes ESPT in order to explain the previous observation[4] of two distinct fluorescence bands in the blue and green spectral regions following the absorption of a UV photon. This type of dual fluorescence is a common feature of molecules of this class.[1] The blue or near-UV fluorescence band is thought to arise from the normal form of the molecule, whereas emission from the tautomer is the more strongly Stokes shifted green fluorescence (Figure 1).

Numerous steady-state and kinetic measurements have been made on 3HF in a wide variety of solvent environments and temperatures in order to elucidate the mechanism of the proton transfer.[3-15] In hydrogen-bonding solvents,[5] or in the presence of hydrogen-bonding impurities in nonpolar environments,[7] observation of normal as well as tautomeric fluorescence is observed. This indicates that, under these conditions, proton transfer occurs slowly enough to allow time for emission from the normal form of the molecule. The tautomer fluorescence rise, and hence the ESPT in polar surroundings, show biexponential[5d,8] dynamics with a subpicosecond fast component[12a] and a slower component which corresponds to the decay of the normal emission. The dual ESPT kinetics in polar media are exceedingly sensitive to temperature and the details of the solvent environment and have been ascribed to 3HF–solvent hydrogen-bonded complexes.[5,7,8,12]

In highly purified and dried hydrocarbon solvents, no emission from the normal form of 3HF is observed even at low temperatures,[7] implying rapid ESPT. There is ample experimental evidence that the proton-transfer time in nonpolar media is exceedingly fast; the rise time of the tautomeric fluorescence of 3HF could not be resolved with picosecond time resolution, even in an Ar matrix at 10 K.[10c,12a] Recently, the rate of intramolecular proton transfer in 2-(2′-hydroxyphenyl)benzothiazole (HBT) has been measured to be 170 ± 20 fs,[16] demonstrating the need for femtosecond time resolution to measure ESPT processes.

In this paper, we use picosecond stimulated emission and transient absorption spectroscopy to determine that ESPT in 3HF can be studied by 620-nm transient absorption. We then use femtosecond transient absorption techniques to temporally resolve the rise of the tautomeric state of 3HF at room temperature. We determine the effects of changing solvent environment on the rate of ESPT and describe a picture of solute–solvent interactions which accounts for the observed dynamics.

II. Experimental Section

A. Experimental Procedures. *1. Femtosecond Laser Setup.* The light source for the femtosecond experiments consists of a homebuilt cavity-dumped, colliding pulse modelocked ring laser,[17] amplified in a six-pass bow-tie amplifier[18] pumped by a copper vapor laser (Metalaser). Partial precompensation of the group

(1) Barbara, P. F.; Walsh, P. K.; Brus, L. E. *J. Phys. Chem.* **1989**, *93*, 29.
(2) (a) Vander Donckt, E. *Prog. React. Kinet.* **1970**, *5*, 273. (b) Ireland, J. F.; Wyatt, P. A. H. *Adv. Phys. Org. Chem.* **1976**, *12*, 131.
(3) Sengupta, P. K.; Kasha, M. *Chem. Phys. Lett.* **1979**, *68*, 382.
(4) Frovlov, Yu. L.; Sapozhnikov, Yu. M.; Barer, S. S.; Pagodaeva, N. N.; Tyukavkina, N. A. *Izv. Akad. Nauk USSR Ser. Khim.* **1974**, *10*, 2364.
(5) (a) Woolfe, G. J.; Thistlethwaite, P. J. *J. Am. Chem. Soc.* **1981**, *103*, 6916. (b) Itoh, M.; Tokumura, K.; Tanimoto, Y.; Okada, Y.; Takeuchi, H.; Obi, K.; Tanaka, I. *J. Am. Chem. Soc.* **1982**, *104*, 4146. (c) Itoh, M.; Fujiwara, Y. *J. Phys. Chem.* **1983**, *87*, 4558. (d) Strandjord, A. J. G.; Courtney, S. H.; Friedrich, D. M.; Barbara, P. F. *J. Phys. Chem.* **1983**, *87*, 1125.
(6) Salman, O. A.; Drickamer, H. G. *J. Chem. Phys.* **1982**, *75*, 572. (b) Salman, O. A.; Drickamer, H. G. *J. Chem. Phys.* **1982**, *77*, 3329.
(7) McMorrow, D.; Kasha, M. *J. Phys. Chem.* **1984**, *88*, 2235.
(8) (a) Strandjord, A. J. G.; Barbara, P. F. *Chem. Phys. Lett.* **1983**, *98*, 21. (b) Strandjord, A. J. G.; Barbara, P. F. *J. Phys. Chem.* **1985**, *89*, 2355. (c) Strandjord, A. J. G.; Smith, D. E.; Barbara, P. F. *J. Phys. Chem.* **1985**, *89*, 2362. (d) Brucker, G. A.; Swinney, T. C.; Kelley, D. F. *J. Phys. Chem.* **1991**, *95*, 3190.
(9) (a) Chou, P.; McMorrow, D. P.; Aartsma, T. J.; Kasha, M. *J. Phys. Chem.* **1984**, *88*, 4596. (b) Dzugan, T. P.; Schmidt, J.; Aartsma, T. J. *Chem. Phys. Lett.* **1986**, *127*, 336. (c) Rulliere, C.; Declemy, A. *Chem. Phys. Lett.* **1987**, *134*, 64.
(10) (a) McMorrow, D.; Dzugan, T. P.; Aartsma, T. J. *Chem. Phys. Lett.* **1984**, *103*, 492. (b) Itoh, M.; Fujiwara, Y.; Sumitani, M.; Yoshihara, K. *J. Phys. Chem.* **1986**, *90*, 5672. (c) Dick, B.; Ernsting, N. P. *J. Phys. Chem.* **1987**, *91*, 4261.
(11) Ernsting, N. P.; Dick, B. *Chem. Phys.* **1989**, *136*, 181.
(12) (a) Brucker, G. A.; Kelley, D. F. *J. Phys. Chem.* **1987**, *91*, 2856. (b) Brucker, G. A.; Kelley, D. F. *J. Phys. Chem.* **1989**, *93*, 5179.
(13) (a) Brewer, W. E.; Studer, S. L.; Standiford, M.; Chou, P. *J. Phys. Chem.* **1989**, *93*, 6088. (b) Brewer, W. E.; Studer, S. L.; Chou, P. *Chem. Phys. Lett.* **1989**, *158*, 345. (c) Sepiol, J.; Kolos, R. *Chem. Phys. Lett.* **1990**, *167*, 445. (d) Martinez, M. L.; Studer, S. L.; Chou, P. *J. Am. Chem. Soc.* **1990**, *112*, 2427.
(14) (a) Parthenopoulos, D. A.; Kasha, M. *Chem. Phys. Lett.* **1990**, *173*, 303. (b) Sarkar, M.; Sengupta, P. K. *Chem. Phys. Lett.* **1991**, *179*, 68.
(15) Dick, B. *J. Phys. Chem.* **1990**, *94*, 5752.
(16) Laermer, F.; Elsaesser, T.; Kaiser, W. *Chem. Phys. Lett.* **1988**, *148*, 119.
(17) (a) Fork, R. L.; Greene, B. I.; Shank, C. V. *Appl. Phys. Lett.* **1981**, *38*, 671. (b) Valdmanis, J. A.; Fork, R. L. *IEEE J. Quantum Electron.* **1986**, *QE-22*, 112.
(18) Knox, W. H.; Downer, M. C.; Fork, R. L.; Shank, C. V. *Opt. Lett.* **1984**, *9*, 552.

0022-3654/92/2096-3591$03.00/0

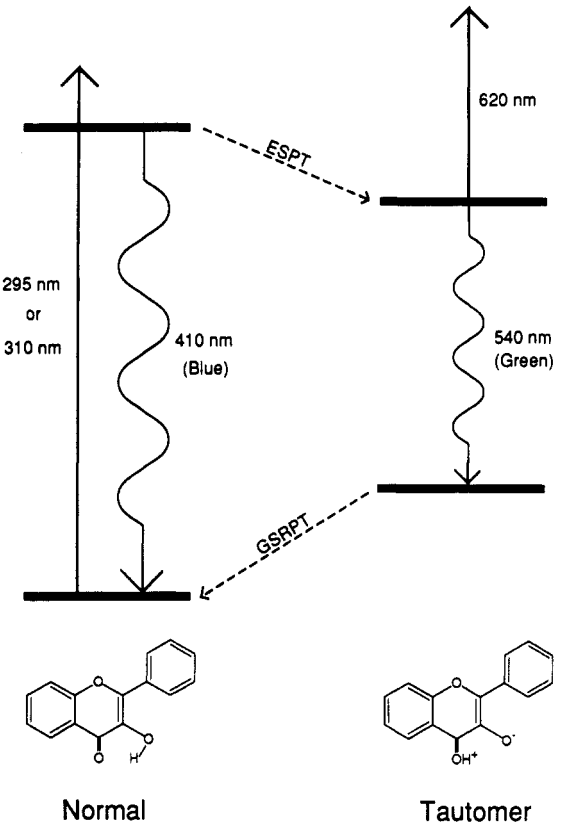

Figure 1. Energy schematic for 3HF. UV excitation of normal 3HF leads to either blue fluorescence or excited-state proton transfer (ESPT). After ESPT, excited tautomers emit green fluorescence and undergo subsequent ground-state reverse proton transfer (GSRPT). Formation of excited 3HF tautomers can be monitored by 540-nm emission or 620-nm absorption.

velocity dispersion in the amplifier and experimental optics can be accomplished by careful adjustment of the prisms in the oscillator. With this excess negative dispersion, the oscillator produces 90-fs pulses dumped at an 8-kHz repetition rate. Timing between the oscillator, cavity dumper, and copper vapor laser is controlled by a digital delay generator (SRS DDG535) and standard NIM electronics. The final light output consists of 620-nm, 100-fs, 3-μJ pulses at 8 kHz. This light is focused into a thin (300 μm) KDP crystal to produce 400-nJ pump pulses at 310 nm. The residual fundamental light is attenuated by neutral-density filters to provide probe pulses with energies of a few nJ.

The 310-nm pump light was passed through a variable delay stage with 1 μm resolution (Klinger MT150) before arriving at the sample. The probe light was split into signal and reference beams, collected on large area photodiodes (EG&G DT-110), and processed by a 386 computer-controlled gated integrator (LeCroy CAMAC 2323, 4300, and 4301). Probe light levels outside a preset range were rejected from data collection. Normalization of the data was achieved on every laser shot; the typical spread ($\pm$1 standard deviation) in the normalized ratios for 100 shots was 0.2%.

Transient absorption data was collected in the following manner: 250 normalized laser shots were averaged for a single data point, the delay between the pump and probe pulses was varied, and then another 250 shots were averaged at the new stage position until an entire scan was completed; 10–40 of these scans (2500–10 000 averaged laser shots) were averaged together in the results presented below, with the stage moving in opposite directions every other scan to account for any forms of long-term drift.

The pump and probe beams crossed through the sample at a 10° angle; this prevented the formation of photoproducts where the pump beam intersected the cell wall from affecting the probe normalization. The beams were focused into the sample with a 15 cm focal length lens, giving an estimated focal spot size of 50 μm. Typical signal sizes were changes in absorbance on the order of 1%. The observed signals were found to vary linearly in size with pump pulse intensity and were independent of the probe intensity, indicating that signals were not due to multiphoton processes. Blanks were run on the pure solvents and no signals were detected.

Polarization experiments were performed with a half-wave plate used to rotate the probe polarization relative to that of the pump. These experiments, and the effect of the half-wave plate on the time resolution of the instrument, are described in detail in Appendix I. The experiments reported below were performed without the half-wave plate, leaving the relative polarizations of the pump and probe beams perpendicular, as produced by type II doubling in KDP.

2. Picosecond Laser Setup. The light source used for the picosecond transient absorption and stimulated emission experiments has been described previously.[19] Briefly, a mode-locked argon ion laser synchronously pumps a dye laser to produce 1–2-ps pulses at 590 nm. These pulses are amplified in a three-stage dye cell amplifier pumped by a 10-Hz, Q-switched Nd:YAG laser. Final output consists of pulses $\sim$1 ps in duration with $\sim$1 mJ/pulse at 10 Hz. The light is doubled in a 1 mm thick KDP crystal, producing 0.1-mJ, 295-nm pump pulses. The residual fundamental light is focused into a 5-cm cell containing water or acetone to generate a white-light picosecond continuum. Ten-nanometer band-pass interference filters are used to select a portion of the continuum to use as the probe light. Data collection is performed in a manner similar to that described above.

The pump and probe beams passed through the sample collinearly. Care was taken to run blank measurements on the neat solvent samples; large pump intensities can produce multiphoton ionization in pure solvents, resulting in large transient absorption signals from solvent cations and/or solvated electrons. Pump power intensity was attenuated with neutral-density filters until no transient signals were observed in the neat solvents. Typical pump pulse energies used in the experiments were 3–8 μJ. The addition of a strong UV absorbing species (like 3HF) should further prevent interfering signals from the solvents. Typical signal sizes obtained with this system were changes in absorbance or gain on the order of a few percent. There were usually 200–1000 laser shots averaged per point in the data presented below.

B. Materials. Methylcyclohexane (99+%) (MCH) was obtained from Aldrich and purified by drying over $CaSO_4$ and molecular sieves. Dry nitrogen was bubbled through the MCH for at least 1 h prior to use, and the MCH was stored under dry nitrogen between uses. This MCH was free of fluorescent impurities. As pointed out in ref 7, even trace amounts of hydrogen-bonding impurities in nonpolar solvents can have a dramatic effect on the ESPT dynamics of 3HF. Observation of biexponential ESPT kinetics in MCH indicates that our purification efforts were not completely successful in removing all traces of polar contaminants. All of the MCH experiments reported in this paper are thus affected by the trace amounts of hydrogen-bonding substances present. The manner in which these impurities affect the results is discussed at great length in the next section.

3-Hydroxyflavone was obtained from Aldrich and purified by multiple recrystallizations from the purified MCH. Spectroscopic grade methanol (MeOH), free from fluorescent impurities, was obtained from Fisher and used without further purification.

Samples were 20 mL of 5×10^{-5}–5×10^{-4} M 3HF/MCH or 3HF/MeOH solution, flowed at $\geq$5 mL/min through a 1 mm $\times$ 1 mm quartz cell (Hellma) with a peristaltic pump (Cole-Parmer) and Viton tubing. This ensured that a fresh sample volume was being probed every laser shot at 10 Hz, and every few laser shots at 8 kHz. The air-tight solution reservoir was continuously purged with dry nitrogen throughout the course of the experiment. All experiments were performed with the samples at room temperature. UV–visible absorption spectra of the

(19) (a) Harris, A. L.; Berg, M.; Harris, C. B. *J. Chem. Phys.* **1986**, *84*, 788. (b) Berg, M.; Harris, A. L.; Brown, J. K.; Harris, C. B. *Opt. Lett.* **1984**, *9*, 50.

TABLE I: Fit Parameters to Picosecond Absorption/Emission Scans[a]

solvent	wavelength,[b] nm	fast rise time, ps	slow rise time, ps	decay time, ns	fast/slow amp ratio
MCH	540	<1.0	9.8 ± 0.4	3.9 ± 0.5	1.4 ± 0.2
MCH	620	<1.0	10.0 ± 0.3	4.0 ± 0.2	1.2 ± 0.2
MeOH	540	<1.0	10.4 ± 0.3	0.28 ± 0.04	−1.8 ± 0.2[c]
MeOH	620	<1.0	10.2 ± 0.3	0.27 ± 0.03	0.4 ± 0.1

[a] Uncertainties based on quality of fit to double-exponential rise, single-exponential decay. [b] 540-nm scans are stimulated emission; 620-nm scans are absorption. [c] Transient absorption decaying into slower stimulated emission.

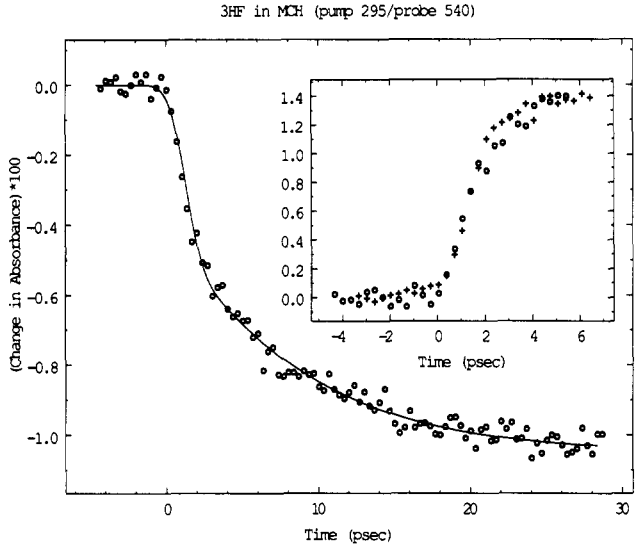

Figure 2. Transient 540-nm stimulated emission of 3HF in MCH. Line is fit given by parameters in Table I, and circles are data points. Inset: Scaled stimulated emission data (circles) overlaid on instrument function (crosses). The fast stimulated emission rise is not time resolved.

samples did not show any significant changes before and after exposure to ultraviolet light.

III. Results

A. Picosecond Transient Absorption and Stimulated Emission. In order to probe the dynamics of ESPT, we used time-resolved stimulated emission spectroscopy to observe the growth of the green tautomer fluorescence (Figure 1). 3HF is excited with the picosecond laser second harmonic at 295 nm, and the tautomer fluorescence buildup is probed at a variable delay with a green picosecond pulse. To more directly compare our results to previous fluorescence[5,8] and stimulated emission[9] work done with poorer time resolution, we chose a probe wavelength of 540 nm. The data are plotted as the change in absorbance of the sample, or $\Delta A = -\log [I/I_0]$ (I_0 is intensity of the probe pulse before the sample, I is intensity of the probe pulse after passing through the sample) as a function of delay time between the pump and probe pulses. Since there are no ground-state tautomer molecules initially present, formation of excited-state tautomers by ESPT leads to a population inversion. The 540-nm probe pulses can undergo gain as they pass through the sample since they are amplified by stimulated emission, leading to negative changes in absorbance. All the data are fit to a dual-exponential rise and single-exponential decay, convoluted with a 1.1-ps Gaussian representing the instrument function. The results of all the fits are summarized in Table I.

A typical picosecond transient stimulated emission scan of 3HF in MCH is shown in Figure 2. The emission shows a dual rise, with the slower rise component comprising 35% of the total gain signal. Comparison of the fast rise time to the instrument function (transient absorption of diphenylbutadiene (DPB) in hexane) shows that the fast rise component is not time resolved (Figure 2, inset). Assuming a δ-function response in DPB, our instrument function fits nicely to the convolution of two 0.8-ps Gaussian pulses. Thus, the tautomer fluorescence rise time, and hence the fast ESPT

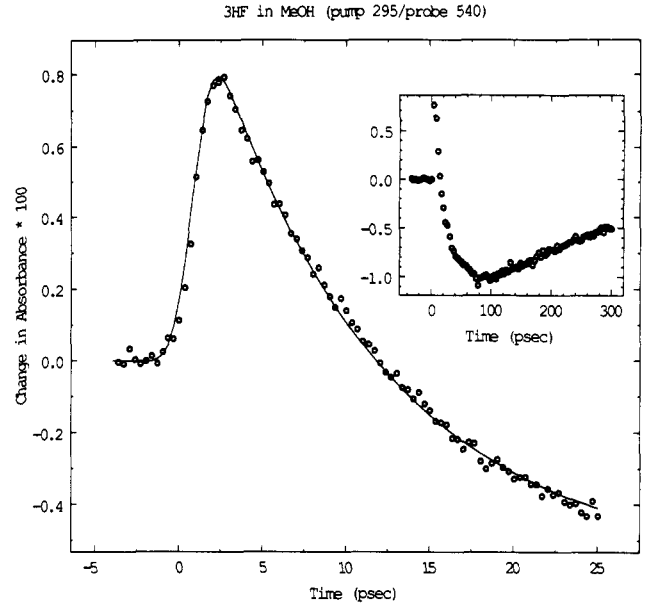

Figure 3. Transient 540-nm stimulated emission of 3HF in MeOH. Line is fit given by parameters in Table I, and circles are data points. Inset: Longer time scan of same sample.

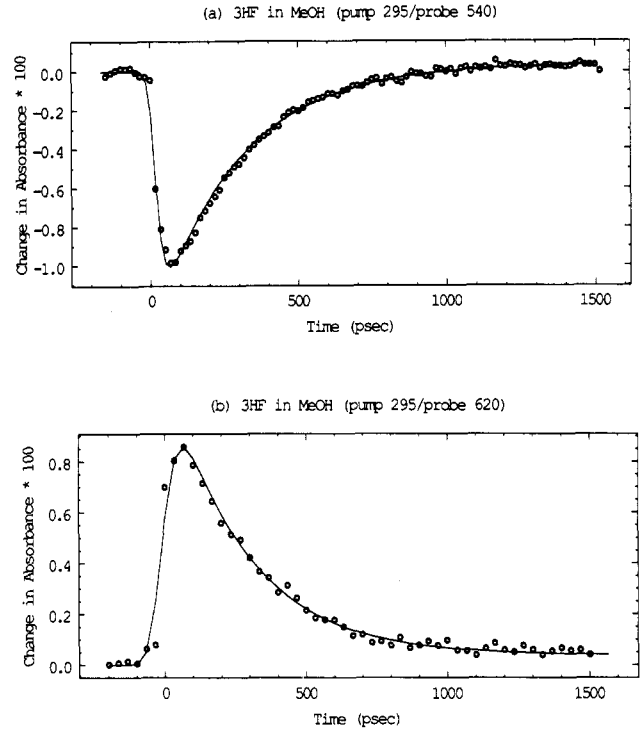

Figure 4. (a) Long-time scan of transient 540-nm stimulated emission of 3HF in MeOH. (b) Long-time scan of transient 620-nm absorption of 3HF in MeOH. Circles are data points, and lines are fits given by parameters in Table I.

time, must be significantly faster than 1 ps at room temperature. This extends previous upper limits obtained at low temperatures.[10,12a]

Picosecond stimulated emission spectroscopy also allows measurement of the fluorescence lifetime of the 3HF tautomer in MCH. Long-time scans show the emission decays in 4.0 ± 0.2 ns (Table I), in good agreement with previous room temperature, tautomer fluorescence lifetime measurements of 4.6,[5a] 3.0,[5c] and 4.0[9b] ns.

The results of experiments studying the tautomer formation dynamics of 3HF in MeOH solutions are shown in Figure 3. The scans show a quickly rising transient absorption at 540 nm, decaying into a more slowly rising (10.4 ± 0.4 ps) stimulated emission. The stimulated emission then exponentially decays in

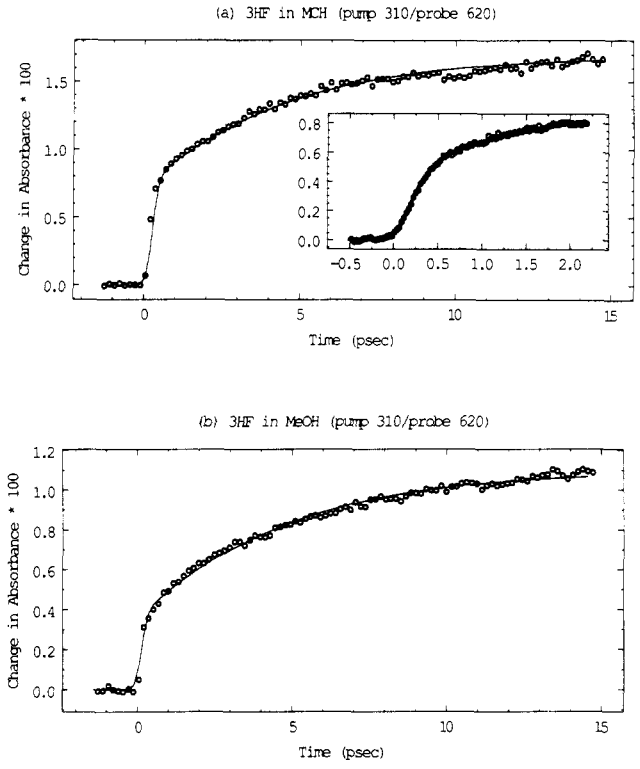

Figure 5. (a) 620-nm transient absorption of 3HF in MCH. Line is fit given by parameters in Table II, and circles are data points. Inset: Shorter time scan—fit is given by parameters in Table III (see text). (b) 620-nm transient absorption of 3HF in MeOH; fit parameters given in Table II.

280 ps (Figure 3, inset; Figure 4a). Due to the large step size, the effective time resolution of the scans of Figure 4 is 35 ps; hence, the fast transient absorption at 540 nm does not appear. The traces of Figure 4 compare well with fluorescence up-conversion experiments taken with similar time resolution (Figure 3b of ref 8b).

All the results indicate that the fast ESPT occurs too quickly to be observed with picosecond time resolution at room temperature. This demonstrates the need to study the tautomer formation with femtosecond time resolution. The femtosecond laser system in our laboratory is limited to probe wavelengths near 620 nm. If the 3HF tautomer excited state has good overlap with an even more highly excited ($\sim$16 000 cm^{-1} higher) tautomer electronic state, then it should be possible to probe the tautomer formation by transient absorption spectroscopy at 620 nm in the same manner as stimulated emission (Figure 1). The transient absorption of 3HF in MCH at 620 nm shows identical dynamics to that observed in stimulated emission (Table I). The long-time transient absorption and emission scans of 3HF in MeOH also reflect identical dynamics (Figure 4). These identical kinetics at 540 and 620 nm indicate that the two wavelengths are probing the same electronic state of the 3HF tautomer.

The assignment of the 620-nm transient absorption to the tautomer excited state has been discussed by others.[9b,c,14a,15] Several groups have studied the transient absorption spectrum of 3HF with $\sim$30-ps time resolution[9] and have presented conflicting results in the rise kinetics and assignments of some of the observed bands. For example, Rulliere and Declemy[9c] reported a rise of the 620-nm absorption band on a 100-ps time scale, and also reported the presence of an initial transient absorption at 500–560 nm for 3HF in MCH. This contradicts the results of Dzugan et al.,[9b] who, in agreement with our results, found the 620-nm absorption rise time faster than their instrumental limit and detected only stimulated emission present between 500 and 580 nm. Despite their differences, both authors concluded that the 620-nm absorption is from the tautomer excited state.[9b,c] This assignment is further supported by recent theoretical work in which the positions of the various electronic states of 3HF and the strengths of the transitions between them were computed.[15] The calculation found no transitions of any significant intensity from the excited normal form of 3HF; in addition, good overlap was computed for the $S_1 \rightarrow S_7$ transition, near 620 nm, of the tautomer. Thus, ESPT in 3HF can be studied by monitoring the tautomer formation with transient absorption spectroscopy at 620 nm.

TABLE II: Fit Parameters to Femtosecond 620-nm Absorption Scans[a]

solvent	fast rise time, fs	slow rise time, ps	fast/slow amp ratio
MCH[b]	210 ± 30	9.3 ± 0.5	1.34 ± 0.2
MCH + drop of MeOH	160 ± 30	9.7 ± 0.5	0.69 ± 0.2
MCH sat. by MeOH	110[c]	10.2 ± 0.5	0.49 ± 0.15
MeOH	80[c]	10.0 ± 0.3	0.42 ± 0.10

[a] Uncertainties based on quality of fit to double-exponential rise. [b] MCH has residual hydrogen-bonding impurities; see text. [c] Rise time is less than 125-fs instrument function.

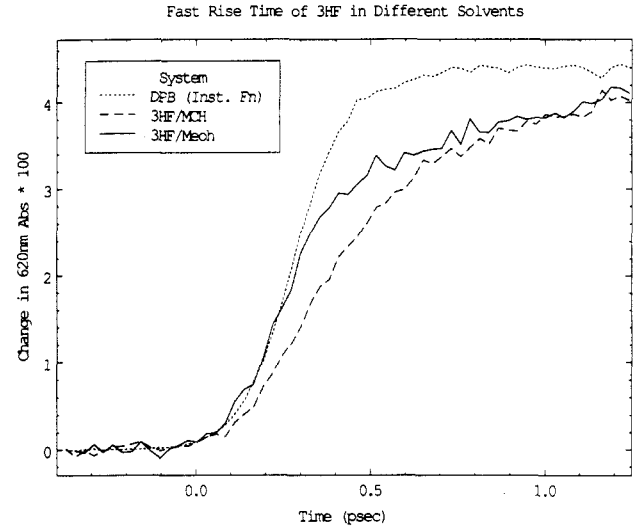

Figure 6. Fast 620-nm absorption rise of 3HF in different solvents. Lines connect the raw data points; dotted is the instrument function, dashed is 3HF in MCH; solid is 3HF in MeOH. All three scans have been scaled to have the same absorbance at a delay of 1.5 ps (see text).

B. Femtosecond Transient Absorption. To elucidate the very fast dynamics of ESPT in 3HF, we performed femtosecond transient absorption measurements. 3HF was excited with the laser second harmonic at 310 nm, and the tautomer formation probed at 620 nm (Figure 1) with the laser fundamental. Typical scans for 3HF in MCH and MeOH are shown in Figure 5. The effects of the solvent environment on the ESPT, as well as the effects of varying the relative polarizations of the pump and probe pulses also have been investigated. The polarization experiments are described in the Appendix. All of the data are fit to a dual-exponential rise convoluted with a 125-fs Gaussian representing the instrument function. The results of all the fits are summarized in Table II.

1. Investigation of Fast Rise Times. The fast transient absorption rises of 3HF in MeOH and MCH were measured with stage steps of 4 μm, or 27 fs/point (Figure 5a, inset). To determine if the fast rise, and hence the fast ESPT, is time resolved, these spectra have been rescaled to have the same absorbance at a delay of 1.5 ps, and superimposed on the instrument function (transient absorption of DPB in hexane) in Figure 6. The fast absorption rise of 3HF in MCH is time resolved, while the fast rise in MeOH is indistinguishable from the instrument function. The fast portion of the MCH rise fits to a 210-fs exponential rise convoluted with the 125-fs Gaussian instrument function; the unresolved fast rise in MeOH fits to the instrument function convoluted with an 80-fs exponential rise (Table II). The slow rise times, visible in Figure 6 as a lowering of the 3HF absorptions below that of the instrument function, are essentially the same in both solvents.

2. Effect of Hydrogen-Bonding Impurities in MCH. The presence of stoichiometric amounts of hydrogen-bonding impurities can drastically alter the ESPT kinetics of 3HF in nonpolar solvents.

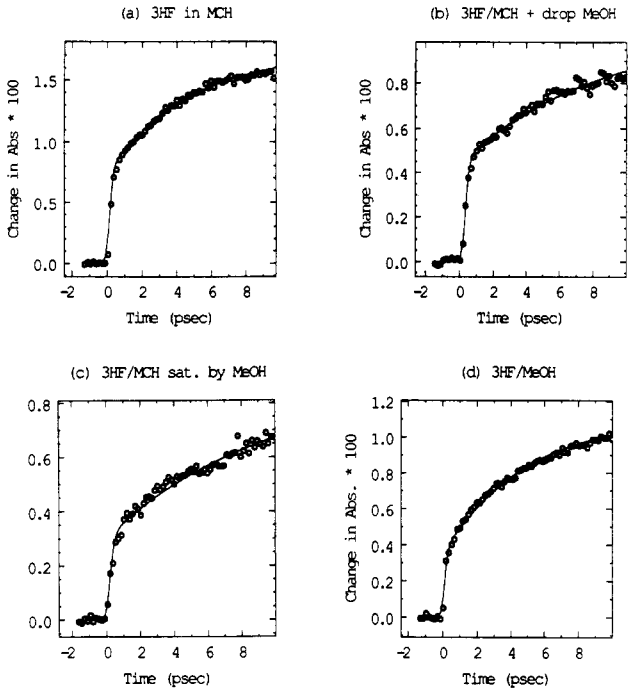

Figure 7. Effect of MeOH addition on 620-nm absorption dynamics of 3HF in MCH. Circles are data points, and lines are fits with parameters given in Table II. (a) 3HF in MCH. (b) Same solution with one drop of MeOH added. (c) Same solution saturated with MeOH. (d) 3HF in pure MeOH.

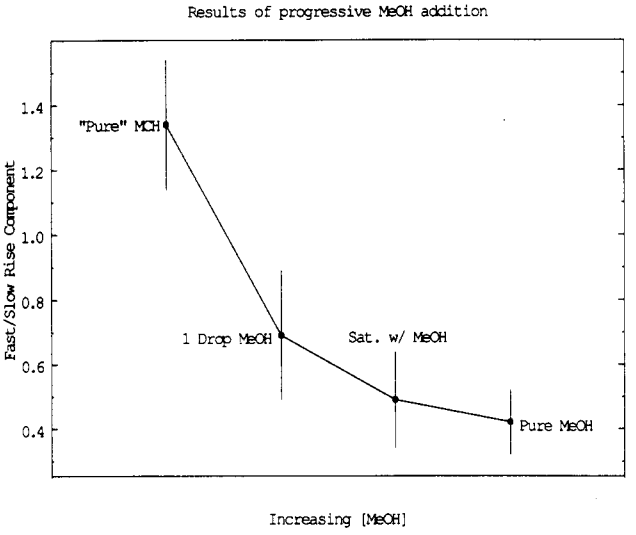

Figure 8. Effects of progressive MeOH addition on the ratio of fast/slow rise components of 620-nm transient absorption of 3HF. Error bars based on uncertainty in fits (Table II). MeOH concentration increases along the horizontal axis.

Following the examples of McMorrow and Kasha[7] and Brucker and Kelley,[12a] we hoped to better understand the effects of these impurities on the transient absorption spectra by intentionally introducing small amounts of MeOH into the MCH solutions. The results of progressive MeOH addition on the transient absorption of 3HF in MCH are shown in Figure 7. The upper left portion of the figure shows the ESPT kinetics of 3HF in pure MCH. The lower right trace is for 3HF in pure MeOH. The trace in the upper right corner was taken after one drop (~0.02 mL) of MeOH was injected into the MCH solution through a 20 gauge syringe needle. The lower left scan shows the effect of saturating the MCH solution with MeOH.[20] The effects of

(20) We refer to an MCH solution as saturated with MeOH when the solution has turned cloudy or has a visible boundary between MCH and MeOH layers.

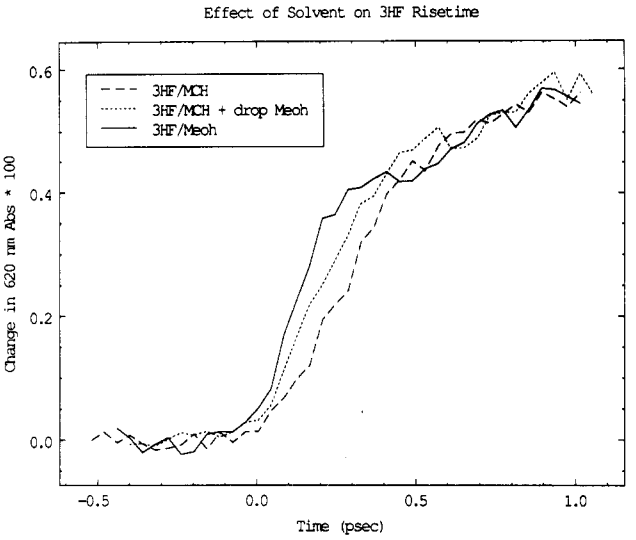

Figure 9. Effect of progressive MeOH addition on fast rise of 620-nm absorption of 3HF. Lines connect the raw data points: dashed is in MCH, dotted is in MCH + one drop of MeOH; solid is in pure MeOH.

TABLE III: Fit Parameters Accounting for Impurities in MCH[a]

rise time component	rel amplitude
10.0 ps[b]	1.0[c]
80 fs[b]	0.42[b]
240 ± 50 fs	0.95 ● 0.15

[a] Fit shown in Figure 5a (convoluted with 125-fs Gaussian); Data fits equally well to double-exponential rise (parameters in Table II); see text. [b] These parameters fixed from fits to pure MeOH data (Table II). [c] Absolute amplitude for 10-ps component picked by best fit to data.

MeOH addition are clear; as more MeOH is added, the ratio of the fast ESPT component to the slow ESPT component decreases, until the MeOH saturated MCH solution has virtually identical kinetics to the pure MeOH solution. This result is summarized in Figure 8 and Table II.

Progressive MeOH addition also has a pronounced effect on the fast ESPT process of 3HF in MCH, as shown in Figure 9 and summarized in Table II. The fast ESPT in MCH is clearly time resolved; addition of one drop of MeOH decreases the rise time significantly; additional MeOH reduces the rise time to that of the pure MeOH solution which is indistinguishable from the instrument function. Since the presence of the slow rise in MCH indicates that there are hydrogen-bonding impurities present,[7] the fast rise in MCH will also be affected by these impurities. Because the fast ESPT in hydrogen-bonding environments is faster than in MCH, the true fast ESPT rate in MCH must be slightly slower than the rate measured above.

The measured fraction of slow/fast ESPT in pure MeOH can be used to correct for the effect of hydrogen bonding impurities on the fast rise in MCH. Because the MeOH results have a fast:slow kinetic component ratio of 0.42, and since 43% of the MCH transient absorption is due to the slow kinetic component, ~18% of the total absorption signal is a fast rise due to MeOH-like impurities. This means that roughly 1/3 of the 57% of the absorption due to the fast rise component is the result of the hydrogen-bonding contaminants. By refitting the MCH transient absorption to account for the known ratio and rise times of the H-bonding impurities, the intrinsic rise time for the pure MCH solvent can be obtained. The fit in the inset of Figure 5a has three exponential rises; the fit parameters are summarized in Table III. Two of the rises are fixed to have the same time constants and amplitude ratio as the fit to the pure MeOH data (Table II). They are scaled appropriately to fit the slow rise of the MCH transient absorption, and convoluted with the 125-fs Gaussian instrument function. Since these parameters are fixed, the remaining rise of 240 fs must be due to the inherent proton transfer rate in MCH. We estimate an uncertainty of ±50 fs for this figure based on the

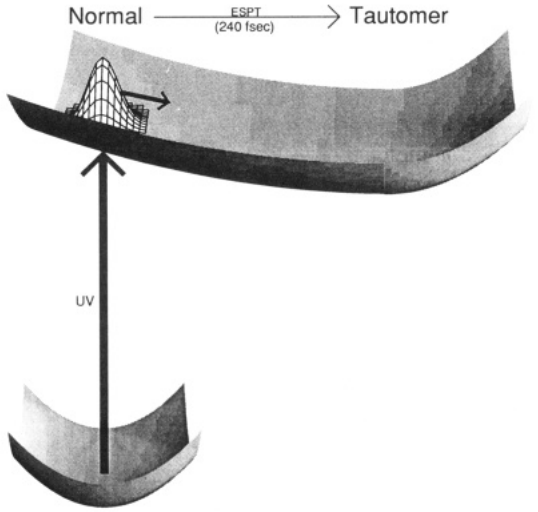

Figure 10. Schematic illustration of wavepacket motion leading to ESPT. The ground-state wave function is displaced from equilibrium on the excited surface; subsequent motion along the reaction pathway leads to tautomerization; displacements along other coordinates do not lead directly to product formation (see text).

uncertainties in the fits to the data and error propagation in the deconvolution. Since a portion of the directly measured 210 fs rise time is pulse-width limited from the impurities, the deconvoluted time of 240 fs is slower than that directly measured, as expected.

IV. Discussion

A. Measurement of Intrinsic ESPT: Fast Rise in MCH. We clearly have time resolved the 210 fs fast exponential rise of the excited tautomer absorption in MCH (Figure 7). As was seen in the early studies,[5,8a] we observe biexponential dynamics for the ESPT of 3HF in MCH. On the basis of experiments of McMorrow and Kasha,[7] and the results of others who found only single exponential tautomer fluorescence rises in nonpolar surroundings,[10a,10c,12a] we assign the slow rise in our results to the presence of hydrogen-bonding impurities in our solvent. The identical rates of the slow component in both MeOH and MCH support this assignment of the slow rise to alcohol-like impurities in MCH. This is confirmed by the results of the progressive MeOH addition experiments (Figures 8 and 9, Table II), which show the slow rise amplitude steadily increasing, but the slow rate remaining unchanged as additional hydrogen-bonding impurities are introduced. When accounting for the effects of the hydrogen-bonding impurities on this fast rise (see above), we determine the ESPT rise time to be 240 ± 50 fs. This constitutes the first direct measurement of the intrinsic ESPT rate of 3HF.

This ESPT rate can be compared to that measured for other molecules, such as 2-(2′-hydroxyphenyl)benzothiazole (HBT). From the infrared stretching frequencies of their O–H bonds, it is evident that HBT[21a] has a stronger intramolecular hydrogen bond than 3HF,[21b] so ESPT is expected to occur at a higher rate in this molecule than in 3HF. A recent measurement gave 170 ± 20 fs for the intrinsic ESPT time of HBT.[16] As expected, this time is slightly faster than our measured time of 240 ± 50 fs for 3HF.

The ESPT times for both of these molecules are significantly slower than the vibrational period of an O–H stretch. This suggests that optical excitation of 3HF is not directly to the dissociative region of the O–H interatom potential in the excited state, in agreement with the conclusions of others.[8d,16] Therefore, the reactive pathway for proton transfer involves movement along coordinates other than simple O–H stretching motion. This motion will be along vibrational coordinates which are significantly displaced from their ground-state equilibrium positions following absorption of a UV photon by 3HF. The tautomerization can be visualized as the propagation of a wavepacket comprising all these motions on the multidimensional excited-state potential surface, depicted schematically in Figure 10. The time for the evolution of this wavepacket from the reactant to the product regions of the surface is the time necessary for proton transfer to occur.

In the wavepacket picture proposed by Elsaesser and co-workers to describe ESPT in HBT,[16] the measured 170-fs tautomerization time is interpreted as the period of the vibrational modes displaced upon excitation. We suggest that the multidimensional nature of the excited-state potential surface may complicate this interpretation. The *initial* motion of the wavepacket, determined by the slope of the excited-state potential in the Franck–Condon region, will depend strongly on the nature of the vibrations displaced upon electronic excitation but the subsequent evolution of the wavepacket may not. Therefore, there may not be a simple relationship between the frequency of the modes displaced and the observed time for ESPT. We picture the tautomerization time as controlled by a series of coupled motions which are eventually dissociative in the O–H coordinate, bringing the wavepacket into the product region of the excited-state potential surface after 240 fs.

The 240-fs ESPT time also allows us to comment on the possibility that phenyl twisting plays a part in the proton-transfer process. Phenyl twisting motion could dynamically modulate the ESPT rate by changing the electronic structure of excited 3HF. Structural studies have suggested that the phenyl twist angle may change the energetics of the ESPT process but were not conclusive about the dynamic role of phenyl torsion.[8c] The lack of viscosity dependence of the slow ESPT rate,[8b] and the results of high-pressure experiments,[6] however, indicate that phenyl twisting is not strongly coupled to the ESPT. Since large-amplitude phenyl torsional motion is an order of magnitude slower than the observed ESPT rate,[22] the measured 240-fs ESPT time also supports this hypothesis. The proton transfer in 3HF happens too quickly for electronic changes induced by phenyl rotation to be important in the ESPT.

B. Fast ESPT in MeOH: 3HF Monosolvate. In hydrogen-bonding environments, the ESPT of 3HF changes drastically. Two distinct ESPT channels appear, a time-unresolved fast component, and a slower component which has been extensively studied.[5d,8] The slow ESPT process is thermally activated and has a barrier height of 1.4 kcal/mol in MeOH.[8b] This changes the fluorescence dynamics significantly; molecules which have not yet undergone the slow ESPT can fluoresce in the blue, from the normal configuration of the molecule, or they can tautomerize and fluoresce in the green, leading to a biexponential rise of the green fluorescence. Many authors have ascribed this slow ESPT in hydrogen-bonding environments (or in the presence of H-bonding impurities in nonpolar solvents) to a variety of solvated 3HF species.[5,7,8,12,14] Typical proposed structures for these 3HF-solvent aggregates are pictured in Figure 11. The $3HF(MeOH)_x$ (x = 1 or 2) complexes have been recently isolated in Ar matrices and characterized.[12a] In particular, the 3HF–MeOH monosolvate has been shown to undergo ESPT in less than 10 ps at 15 K.[12a]

The fast excited tautomer absorption rise we measure for 3HF in MeOH is indistinguishable from our instrument function, indicating that the fast ESPT is taking place in ≤125 fs. This suggests that an entirely new motion dominates the ESPT reaction coordinate in MeOH or, in other words, that the fast ESPT takes place by a different mechanism in MeOH than in nonpolar solvents. In the picture of ESPT in nonpolar environments described earlier, *intra*molecular modes displaced upon excitation lead to tautomerization. In polar solvents, the formation of hydrogen-bonded complexes creates new *inter*molecular motions which may play an important role in the tautomerization process. If the new intermolecular modes are also displaced upon excitation, the resulting wavepacket could follow a trajectory on the excited-state

(21) (a) Elsaesser, T.; Schmetzer, B.; Lipp, M.; Bauerle, R. J. *Chem. Phys. Lett.* **1988**, *148*, 112. (b) Pouchet, C. J. *The Aldrich Library of FT-IR Spectra*, 1st ed.; Aldrich Chemical Co.: Milwaukee, WI, 1985; Vol. 2, p 95B.

(22) Ben-Amotz, D.; Harris, C. B. *J. Chem. Phys.* **1987**, *86*, 4856.

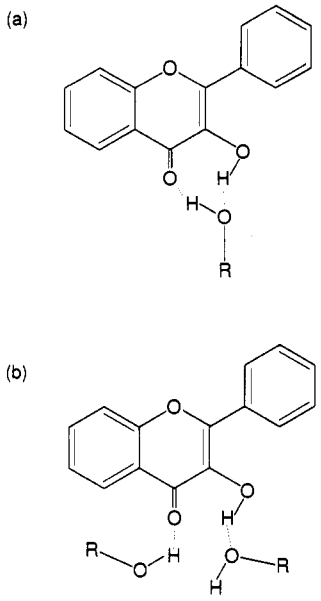

Figure 11. (a) Typical proposed structure for cyclically H-bonded 3HF-MeOH monosolvate. (b) Typical proposed structure for 3HF–MeOH disolvated complex.

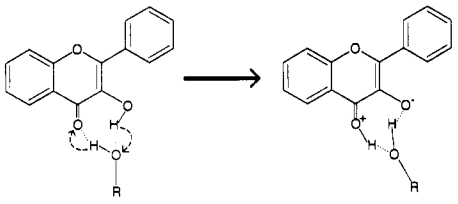

Figure 12. Possible mechanism for dual proton transfer in 3HF–MeOH cyclically H-bonded monosolvate. Arrows indicate relative proton motions upon electronic excitation.

surface which is altered from that of the unsolvated species, leading to a different measured proton-transfer time.

The most likely candidate for this faster, intermolecularly dominated ESPT is the cyclically H-bonded 3HF monosolvate ($3HF(MeOH)_1$)[12a] (Figure 11a). The fast ESPT mechanism for the monosolvated 3HF could involve dual proton transfer. Excitation of the 3HF changes the acidity and basicity of the carbonyl and hydroxy moieties;[2] the now basic carbonyl group can easily accept the closely bound alcohol proton, while the newly acidic hydroxy proton can transfer easily to the deprotonating alcohol. The dual ESPT process is illustrated in Figure 12. This type of double proton transfer has been postulated for several molecules in hydrogen-bonding solvents, including 7-azaindole.[23] Whether this dual transfer process is concerted or sequential cannot be determined from our data.

It is entirely plausible that the dual ESPT in $3HF(MeOH)_1$ is faster than the intrinsic ESPT in the free molecule. The hydrogen bonds in the 3HF solvated complex are likely to be stiffer and, therefore, of higher frequency than the intramolecular hydrogen bond of the unsolvated species. This implies that the wavepacket is composed of higher frequency components in the monosolvate than in free 3HF, leading to more rapid tautomerization. In addition, the stronger intermolecular hydrogen bonds in the solvated complex start the protons closer to their final tautomeric positions than the weaker intramolecular hydrogen bond in isolated 3HF, suggesting that the wavepacket would be propagating for less distance on the intermolecular reaction pathway. If the intermolecular hydrogen bond vibration is important to the monosolvate proton-transfer reaction coordinate, either or both of these observations can be used to rationalize the more rapid evolution of the wavepacket on the excited-state surface of the aggregate than of the isolated molecule.[24] These ideas, and the previously measured 10-ps upper limit for ESPT of the monosolvate at 10 K,[12a] make the ≤125-fs time for a dual ESPT mechanism in $3HF(MeOH)_1$ at room temperature reasonable.

The rapid fast ESPT times for the bare 3HF and monosolvated 3HF species have implications for the mechanism of the slower ESPT process. The slow ESPT has been ascribed to the presence of the 3HF disolvate (Figure 11b). The disolvate itself does not undergo proton transfer,[12a] so the slow ESPT time is a measure of the time for desolvation of $3HF(ROH)_2$ to become either the monosolvated or the free 3HF species. Several models, including thermally activated desolvation,[5a] desolvation followed by rate-limiting proton transfer,[5d,8b] and Marcus-like solvent polarization fluctuations,[8d] have been proposed to describe this process. Whatever the mechanism involved, it seems that proton-transfer time is virtually instantaneous compared to the desolvation time. This is supported by the data of Figure 3, which shows a transient absorption at 540 nm due to $3HF(MeOH)_2$ decaying smoothly into the stimulated emission of the tautomer. The tautomer emission rises with the disolvate absorption decay time; there is no evidence for any type of bottleneck on the picosecond time scale. Whether the subsequent proton transfer occurs from the free 3HF, the monosolvate, or a mixture of the two species, the ESPT happens rapidly once desolvation of the disolvate is complete.

V. Conclusions

We have performed the first investigation of the fast ESPT dynamics of 3HF in alkane and alcohol solvents. Picosecond stimulated emission spectroscopy indicates that the tautomer is formed in less than 1 ps and that the 620-nm transient absorption occurs from the tautomer excited state. By studying this absorption with femtosecond time resolution, the fast ESPT of 3HF has been observed in different solvents.

The appearance of a slow ESPT component in MCH indicates the presence of hydrogen-bonding impurities in solution. The ESPT kinetics in hydrogen-bonding environments were studied in MeOH, and the results were used to account for the effects of the impurities in the MCH solution. The fast ESPT time in MCH was determined to be 240 ± 50 fs; the fast ESPT time in MeOH was faster than the 125-fs instrument response.

The 240-fs time scale for the ESPT in MCH is too long for O–H stretching motion and too short for large-amplitude phenyl torsion to be of major importance in the proton-transfer reaction coordinate. Instead, we describe a model for ESPT based on the evolution of vibrational motions coupled to the electronic excitation; the ESPT time corresponds roughly to the propagation time of the wavepacket comprised of the modes displaced. The faster ESPT time in MeOH solution can be explained by consideration of a 3HF–MeOH cyclically H-bonded complex. The ESPT reaction coordinate in this aggregate comprises new modes resulting from hydrogen motion between the 3HF and the solvent molecules. The higher frequency motions constituting the wavepacket and a shorter overall reaction pathway to travel for tautomerization each contribute to the faster ESPT time in the monosolvate. We suggest that the 3HF monosolvate undergoes ESPT by a dual proton transfer mechanism.

Note Added in Proof. Subsequent experiments on 3DF (deuterated 3-hydroxyflavone) in MCH and 3DF in MeOD found no significant changes in the fast ESPT dynamics upon deuteration. This is in agreement with recent results on deuterated HBT (Frey, W.; Laermer, F.; Elsaesser, T. *J. Phys. Chem.* **1991**, *95*,

(23) (a) Moog, R. S.; Bovino, S. C.; Simon, J. D. *J. Phys. Chem.* **1988**, *92*, 6545. (b) Ingham, K. C.; El-Bayoumi, M. A. *J. Am. Chem. Soc.* **1974**, *96*, 1674.

(24) Alternatively, this process can be viewed as the original wavepacket comprising intramolecular vibrations propagating on an electronic surface that has been altered by interaction with the polar solvent. The Stokes shift of the tautomer fluorescence, however, changes less than 200 cm^{-1} between MCH and MeOH,[8b] implying that the electronic surfaces are not shifted significantly upon polar solvation. Therefore, we prefer the picture of new, intermolecular modes changing the evolution of the wavepacket for 3HF in MeOH.

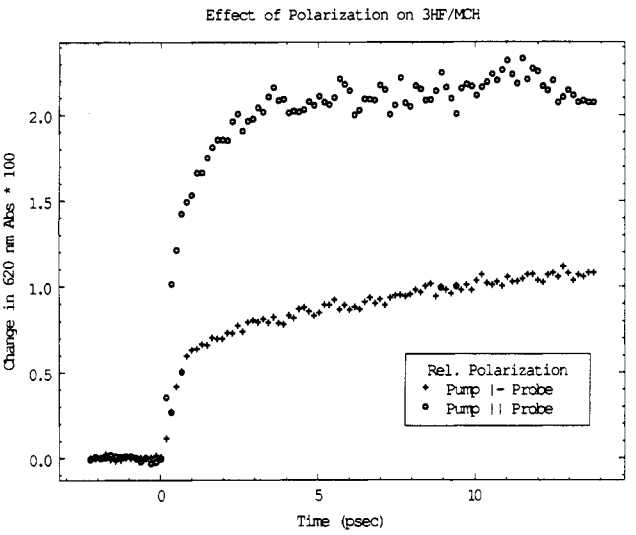

Figure 13. Effects of relative polarization of pump and probe beams on 620-nm transient absorption of 3HF in MCH. Circles are data for parallel polarizations, and crosses are data for perpendicular polarization. Rise times and fast/slow rise amplitude ratios are the same for both scans.

10395) which also found no deuterium isotope effect on the proton transfer rate.

Acknowledgment. We acknowledge many helpful discussions with Dr. Jin Zhang. B.J.S. gratefully acknowledges the support of the National Science Foundation for an NSF graduate fellowship, and the support of W. R. Grace & Co. for a Grace Foundation fellowship. L.A.P. acknowledges the support of NIH postdoctoral training grant T32E4 07043. This work was supported by a grant from the National Science Foundation.

Appendix. Effect of Polarization

To verify that both the fast and slow rise components of the 620-nm transient absorption are due to the tautomer excited state, and to account for the effects of rotational reorientation of the 3HF during the ESPT, we have performed a series of experiments with different relative orientations of the pump and probe pulse polarizations. Figure 13 shows the 620-nm transient absorption kinetics of 3HF in MCH taken with parallel and perpendicular pump/probe polarizations. Neither the rise times nor the fast/slow rise component ratios change with relative polarization. Experiments performed with relative polarization at the magic angle (54.7°) also showed identical results. This indicates that the absorptions of both kinetic components come from the same electronic state of the molecule (or from different states with parallel transition dipoles) and that the effects of rotational diffusion are not important on this time scale. This independence of the dynamics from relative polarization is in agreement with previous emission studies.[5d]

The information of Figure 13 can be used to determine the relative orientations of the transition dipoles of the 3HF ground state and the excited state giving rise to the transient absorption signal. The signal size ratio of 2.3 ± 0.3:1 for parallel:perpendicular orientations indicates that the transition dipole of the tautomer excited state is mostly parallel to that of the initial excitation (the ratio expected for a perfectly parallel transition is 3:1). The anisotropy $A = (I_{\parallel} - I_{\perp})/(I_{\parallel} + 2I_{\perp})$ of this transition is ~0.25, implying an angle of ~20° between the ground-state and the transiently absorbing tautomer excited-state transition dipoles.[25] Since the molecule has undergone ESPT and now has significant zwitterionic character, we would expect the electronic structure of the excited state to be altered significantly from that of the ground state. This makes the result of nearly parallel transition dipoles somewhat surprising, although not completely unlikely. To the best of our knowledge, no one has reported the orientation of the excited-state transition dipole in a molecule that undergoes ESPT. The parallel result, however, is in agreement with recent findings on the tautomer emission dipole orientation of 2-(2′-hydroxyphenyl)benzothiazole (HBT) in nonpolar environments.[26]

Since the transient absorption kinetics are independent of the relative pump and probe polarizations, the experiments can be performed without the use of the half-wave plate needed change the probe polarization. This allows improved time resolution, as noncompensatable dispersion in the half-wave plate broadens the instrument function from 125 to 140 fs. To better resolve the fast rise component in MeOH solutions, the experiments above were performed without the half-wave plate.

Registry No. 3-Hydroxyflavone, 577-85-5; methanol, 67-56-1; methylcyclohexane, 108-87-2.

(25) Cantor, C. R.; Schimmel, P. R. *Biophysical Chemistry Part II: Techniques for the Study of Biological Structure and Function*; W. H. Freeman and Co.: San Francisco, 1980; Section 8-2.
(26) Schwartz, B. J. Unpublished data, 1991.